# IMPACT OF QUANTIZATION ON CHANNEL ESTIMATION IN OFDM COMMUNICATION SYSTEM

Miha Smolnikar, Mihael Mohorcic
Department of Communication Systems
Jozef Stefan Institute
Ljubljana, Slovenia

Haris Gacanin, Fumiyuki Adachi
Graduate School of Engineering
Tohoku University
Sendai, Japan

## ABSTRACT

Orthogonal frequency division multiplexing (OFDM) system with frequency domain equalization (FDE) requires reliable channel estimation (CE). In practice, pilot assisted CE can be either based on time- or frequency-domain multiplexed pilot symbols (i.e. TDM-pilot and FDM-pilot). It this paper, the impact of quantization noise introduced by digital-to-analog (DA) and analog-to-digital (AD) converters is examined. Furthermore, the trade-off between the resolution of DA/AD converters and back-off levels of the DA converter is evaluated. The simulation results are provided in terms of bit error rate (BER) for different configurations of the OFDM system. We show, that TDM-pilot CE scheme requires lower DA and AD converter resolutions than FDM-pilot CE scheme to achieve comparable performance. This is a consequence of pilot symbols' amplitude clipping at the DA converter and/or large amplitudes that need to be covered by AD converter in the case of FDM-pilot CE scheme. This is not the case in TDM-pilot CE scheme, where Chu pilot sequence with constant amplitude of pilot symbols is applied.

## I INTRODUCTION

In a terrestrial wireless channel, a signal typically propagates over a number of different paths that give rise to a frequency-selective fading. This produces inter-symbol interference (ISI) and degrades the transmission performance [1]. To overcome this problem orthogonal frequency division multiplex (OFDM) [2] may be considered. Its main advantages include efficient spectrum utilization and high degree of flexibility since coding, constellation and power assignment can be adaptively controlled per subcarrier according to user requirements and/or changes of the communication environment. But the performance enhancements are most often largely dependent on the accuracy of channel estimation (CE).

In general, there are two approaches to perform the CE [3], one based on time-domain multiplexed pilot symbols (TDM-pilot) and the other on frequency-domain multiplexed pilot signals (FDM-pilot). Schemes of the first approach lack tracking ability against fast, doubly-selective fading, while schemes of the second approach are characterised by increased bit error rate (BER) due to noise enhancement as a consequence of the frequency-domain interpolation.

The main drawback of OFDM is high amplitude fluctuation, i.e. high peak-to-average power ratio (PAPR), which requires large dynamic range and high linearity of system's analog components. In the design of contemporary OFDM systems the main source of nonlinearities is the high power amplifier (HPA) in transmitter, most often mitigated by predistortion and filtering techniques. Another group of critical components introducing nonlinearities are digital-to-analog (DA) converters at the transmitter and analog-to-digital (AD) converters at the receiver. Usually, these are assumed to have a large number of quantization levels and optimally exploited dynamic range. With such assumptions, the quantization noise (representing quantizer granularity) and clipping noise (corresponding to overloading distortion) can be neglected [4]-[6]. However, in order to keep the system complexity and power consumption low, it is desired to keep the DA/AD converters resolution as low as possible [7], [8], particularly in mobile/handheld devices with power constraints.

This paper investigates practical CE schemes in a frequency-selective fading channel, with a particular focus on the system performance degradation as a consequence of DA/AD converters. Quantization introduced by these elements is a nonlinear function applied in the time domain and its effect in the frequency domain is not trivial [9]. Hence, the selection of CE scheme and DA/AD converter configurations is decisive to achieve good performance of the OFDM communication system. The distinctive aspect of this work is the consideration of practical CE schemes, whilst respecting the impact of DA and AD converters as quantizers and amplitude clippers.

The rest of the paper is organized as follows. Section II describes the OFDM system model, with the emphasis given on the DA and AD converter models. Channel estimation schemes are presented in Section III. Performance evaluation results obtained by computer simulations are provided in Section IV. Section V concludes the paper.

## II SYSTEM OVERVIEW

The baseband OFDM system model considered in this study is illustrated in Fig. 1. All blocks, except the DA and AD converters and HPA, are assumed to be linear, and symbol timing is assumed to have no jitter. Throughout this paper, a discrete-time signal representation is used, where $T_c$ denotes the fast Fourier transform (FFT) sampling period and $K$ is the number of subcarriers.

The $n$th frame OFDM complex baseband signal $s(t)$ is obtained as inverse FFT (IFFT) over the $K$ data-modulated symbols $S(k)$ as

$$s(t) = \frac{1}{\sqrt{K}} \sum_{k=0}^{K-1} S(k) e^{j2\pi t \frac{k}{K}}, \quad (1)$$

for $t = 0 \sim K-1$.

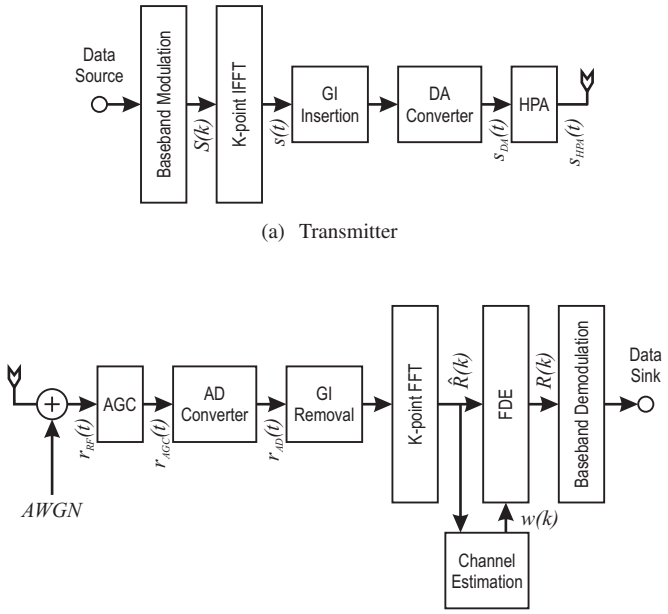


(a) Transmitter

(b) Receiver

Figure 1: OFDM system model.

After the insertion of $K_g$-sample guard interval (GI) the signal is fed to a DA converter, to transform the signal from digital to analog domain. DA conversion is represented by a quantization model as follows. For an $R$ bit resolution DA converter with $M = 2^R$ quantization levels, the signal after DA conversion is expressed as

$$s_{DA}(t) = s^I_{DA}(t) + j s^Q_{DA}(t), \tag{2}$$

where the in-phase ($I$) and quadrature ($Q$) signal components are given as

$$s^I_{DA}(t) = q\left[\Re\left\{s(t)\right\}\right] \tag{3}$$

and

$$s^Q_{DA}(t) = q\left[\Im\left\{s(t)\right\}\right]. \tag{4}$$

In the above equations $q[z]$ represents the quantization function defined as

$$q[z] = \begin{cases} Q_{out} & z > Q_{in} \\ \frac{Q_{out}}{Q_{in}}\left(\left\lfloor \frac{z}{Q_\Delta} \right\rfloor Q_\Delta + \frac{Q_\Delta}{2}\right) & -Q_{in} \le z \le Q_{in}, \\ -Q_{out} & z < -Q_{in} \end{cases} \tag{5}$$

with the $\lfloor \cdot \rfloor$ representing the floor function (i.e. rounding to nearest integer lower or equal to argument) and the quantization step size given by

$$Q_\Delta = \frac{1}{Q_{in}} \cdot \frac{2}{2^R - 1}, \tag{6}$$

where $Q_{in}$ and $Q_{out}$ denote quantizer input and output signal amplitudes respectively.

The analog signal is fed to HPA, where amplification is achieved as $s_{HPA}(t) = \sqrt{2P_{HPA}} s_{DA}(t)$. The transmit signal

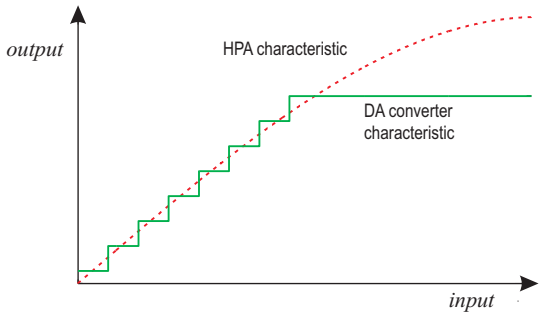


Figure 2: HPA and DA converter input-output characteristics.

power is given as $P_{HPA} = E_s/T_c K$, with $E_s$ denoting data-modulated symbol energy. We assume here that the HPA is exploited in its linear region, thus the maximum output amplitude of DA converter is not exceeding the HPA saturation amplitude level. These conditions are depicted in Fig. 2 through HPA and DA converter characteristic.

The signal is transmitted over a frequency-selective fading channel, with the discrete-time channel impulse response $h(t)$ given as

$$h(t) = \sum_{l=0}^{L-1} h(l)\delta(t - \tau(l)), \tag{7}$$

where $L$ is the number of propagation paths, and $h(l)$ and $\tau(l)$ are the $l$th path gain and delay during the $n$th frame, respectively. We assume the maximum channel delay being lower than the length of GI. The channel transfer function is $H(k) = FFT\left\{h\left(t\right)\right\}$.

At the receiver, the analog received signal $r_{RF}(t)$ is first amplified by the automatic gain control (AGC) as

$$r_{AGC}(t) = P_{AGC} r_{RF}(t), \tag{8}$$

where $P_{AGC}$ is the AGC amplification. Thus, the peak signal amplitude at the AD converter input $A_{AGC,m} = max\left(|r_{AGC}(t)|\right)$ corresponds to its maximum value. This assures minimum quantization and no clipping errors in quantized signal $r_{AD}(t)$, occurring respectively for too small and too large AGC output signals $r_{AGC}(t)$, as depicted in Fig. 3 for sinusoidal signals with different amplitudes. The quantization introduced by the AD converter can also be modelled by Eq. (5) and Eq. (6). The AD converter output signal can be expressed as

$$r_{AD}(t) = q\left[r^I_{AGC}(t)\right] + jq\left[r^Q_{AGC}(t)\right], \tag{9}$$

where $r^I_{AGC}$ and $r^Q_{AGC}$ represent the amplified in-phase and quadrature signal components of the received signal .

After removal of the GI, the signal is fed to FFT. The latter decomposes the signal into $K$ subcarrier components as

$$R(k) = \frac{1}{\sqrt{K}} \sum_{t=0}^{K-1} r_{AD}(t) e^{j2\pi k \frac{t}{K}}, \tag{10}$$

or written in terms of Fourier transforms

$$R(k) = S(k)H(k) + N_{AWGN}(k) + N_Q(k), \tag{11}$$

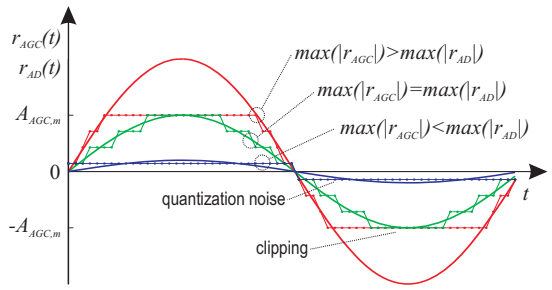


Figure 3: AD converter quantization noise and clipping

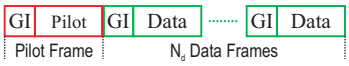


Figure 4: TDM-pilot block insertion.

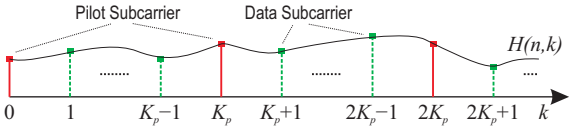


Figure 5: FDM-pilot arrangements

where $N_{AWGN}(k)$ and $N_Q(k)$ denote FFTs of additive white Gaussian noise (AWGN) and quantization noise caused by the use of DA and AD converters, respectively.

To correct the channel distortion on each subcarrier frequency domain equalization (FDE) is applied to $R(k)$ as

$$\hat{R}(k) = R(k)w(k) \tag{12}$$

for $k = 0 \sim K-1$, where $w(k)$ denotes the equalization weight given by

$$w(k) = \frac{H_e^*(k)}{|H_e(k)|^2}. \tag{13}$$

In Eq. (13), $(\cdot)^*$ denotes the complex conjugate operation and $H_e(k)$ denotes the estimate of $H(k)$. CE schemes are described in the following section. Following FDE, the equalized received data symbols $\hat{R}(k)$ are demodulated.

## III Channel Estimation

This section is devoted to the presentation of channel estimation schemes. We are focusing on two schemes [3]: $(i)$ CE using TDM-pilot and $(ii)$ CE using FDM-pilot.

### *III.A CE with TDM-pilot*

In the case of TDM-pilot CE scheme a pilot signal frame is transmitted on all $K$ subcarriers, followed by $N_d$ OFDM data frames, as shown in Fig. 4.

First, by reverse modulation of pilot frame shown in Fig. 4, the instantaneous channel gain estimate $\tilde{H}(k)$ at $k$th subcarrier is obtained as

$$\tilde{H}(k) = \frac{R(k)}{P(k)} = H(k) + \tilde{N}_{AWGN}(k) + \tilde{N}_Q(k) \tag{14}$$

for $k = 0 \sim K-1$, where $\tilde{N}_{AWGN}(k) = \frac{N_{AWGN}(k)}{P(k)}$, $\tilde{N}_Q(k) = \frac{N_Q(k)}{P(k)}$, and $P(k)$ denotes the $k$th subcarrier of time-domain pilot sequence $p(t)$. Then, $K$-point IFFT is applied to $\tilde{H}(k)$ to obtain the instantaneous channel impulse response $\tilde{h}(t)$ for $t = 0 \sim K-1$. Assuming that the actual channel impulse response is present only within the GI, the estimated channel impulse response beyond the GI is replaced with zeros to reduce the noise [10]. Finally, $K$-point FFT is applied to obtain the improved channel gain estimates $H_e(k)$ for $k = 0 \sim K-1$.

For an accurate channel estimation, the selection of appropriate pilot sequence is very important. In order to avoid AWGN and quantization noise enhancements it is thus desired that $P(k)$ has constant amplitude irrespective of $k$, which on the contrary leads to large amplitude variations of $p(t)$ and potential degradations due to non-linear amplification and/or DA conversion. To achieve constant amplitudes in both time- and frequency-domain, this study considers the use of Chu pilot sequence [11], given as

$$p(t) = \cos(n\pi t^2/K) + j\sin(n\pi t^2/K), \tag{15}$$

for $t = 0 \sim K-1$.

### *III.B CE with FDM-pilot*

In CE scheme with FDM-pilot a high-order frequency domain interpolation is used over $K_p$ equally-spaced pilot subcarriers, which represent a subset of the $K$ subcarriers.

First, by reverse modulation, the instantaneous channel gain estimate $\tilde{H}(k)$ is obtained by Eq. (14) at $k = \left\lfloor \frac{p}{K_p} \right\rfloor$ pilot subcarriers, for $p = 0 \sim K-1$. Channel gain estimates are thus obtained only at frequencies $k = 0, K_p, 2K_p, \ldots, (K-1)$ as depicted in Fig. 5. Then, $K_p$-point IFFT is performed to obtain instantaneous channel impulse response $\tilde{h}(t)$ for $t = 0 \sim K_p - 1$. Finally, to obtain channel gain estimates $H_e(k)$ for all $k = 0 \sim K-1$ subcarriers, $K$-point FFT is applied to $\tilde{h}(k)$.

## IV Computer Simulations

Performance evaluation results in Subsections IV.A, IV.B and IV.C are provided in terms of BER for different CE schemes and DA/AD converter configurations. The results were obtained by computer simulations, with the simulation parameters summarized in Table 1. We adopt QPSK data-modulation with $K = 256$ and $K_g = 16$. The data and pilot symbols are always being sampled with the same DA/AD coverter resolutions. The propagation channel is a $L$=8-path frequency selective block Rayleigh fading having the exponential power delay profile. At the receiver, perfect synchronization, ideal AGC and zero-forcing (ZF) FDE are considered.

### *IV.A BER Performance for Different CE Schemes*

The average BER performances as a function of signal energy per bit to AWGN spectrum density ratio, defined as $E_b/N_0 =$

Table 1: Simulation parameters.

| | | |
|---|---|---|
| Transmitter | Data modulation | QPSK |
| | IFFT size | $K=256$ |
| | GI | $K_g=16$ |
| Channel | $L$=8-path Rayleigh fading | |
| Receiver | FDE | ZF |
| | CE | TDM- and FDM-pilots |

$0.5 \cdot (E_s/N_0)(1+K_g/K)$, are for OFDM models with ideal, TDM-pilot and FDM-pilot CE schemes and different resolutions of DA and AD converters depicted in Fig. 6, Fig. 7 and Fig. 8, respectively. The results were obtained for the input back-off of the DA converter ($IBO_{DA}$) set to 10 dB. The effect of the quantization noise initiated by DA and AD converters produces so called error floors (i.e flattening of the original BER curves), increasing the achievable BER for the decreasing DA/AD converter resolution. We consider the target BER being $10^{-4}$ and provide the results only for the minimum required DA/AD resolution to respect this criterion. The latter is for ideal CE and infinite DA and AD converter resolution during pilot and data transmission fulfilled at $E_b/N_0 = 34.0$ dB, representing the theoretical boundary. For TDM-pilot CE scheme this value increases to 35.6 dB, and for FDM-pilot CE scheme to 37.3 dB.

The results in Fig. 6 were obtained for ideal CE and show that 3 bit DA converter and 7 bit AD converter resolutions nearly provide the targeted performance. The results for the TDM-pilot CE scheme are provided in Fig. 7, and show that a higher DA converter resolution is required to achieve comparable performance. In particular, the DA and AD converter resolutions should respectively equal to at least 4 and 7 bits. Finally, for the case of FDM-pilot CE scheme, the results are depicted in Fig. 8, and denote this scheme requires highest DA and AD converter resolutions. The BER $= 10^{-4}$ can be achieved with 6 bit DA converter and 8 bit AD converter resolution.

### *IV.B The Impact of Bit Resolution*

For a system with infinite DA and AD converter resolution, the target BER $= 10^{-4}$ criterion is fulfilled at $E_b/N_0$ approximately equal to 35 dB. This value was thus selected as a parameter for the analysis of BER dependence on the resolution of DA and AD converters. The results in Fig. 9 are provided for all three CE schemes (i.e. ideal, TDM-pilot and FDM-pilot), separate inclusion of DA or AD converter and the DA converter input back-off $IBO_{DA} = 10$ dB.

For a particular OFDM system and propagation conditions the FDM-pilot CE scheme is significantly more sensitive to quantization noise than the TDM-pilot CE scheme, which practically corresponds to the ideal CE. This is a consequence of pilot symbols amplitude clipping at DA converter and/or large amplitudes that need to be covered by AD converter and the consequent large quantization steps in the case of FDM-pilot CE scheme. In TDM-pilot CE scheme this is not the case, as

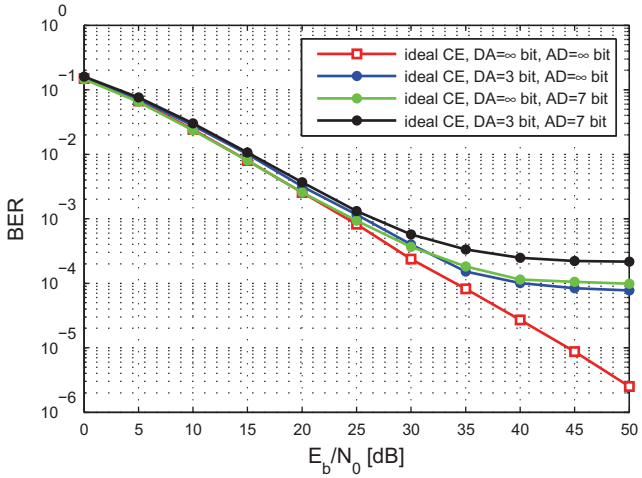


Figure 6: BER performance for ideal CE

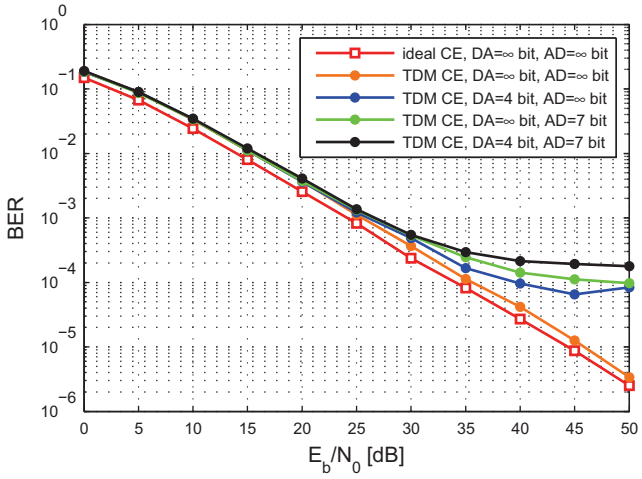


Figure 7: BER performance for TDM-pilot CE

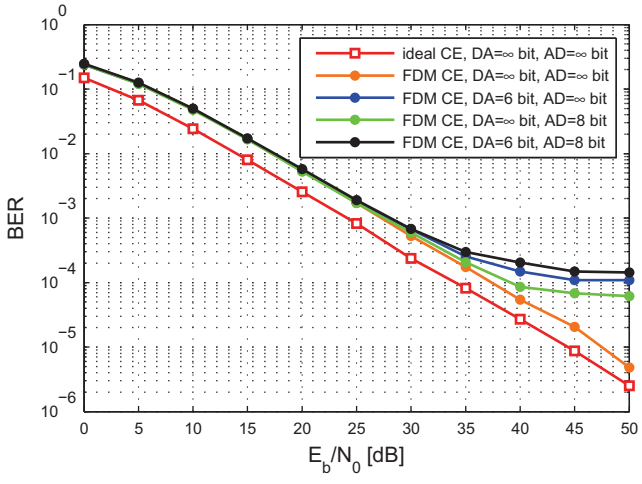


Figure 8: BER performance for FDM-pilot CE

Chu pilot sequence characterised by a constant amplitude is applied.

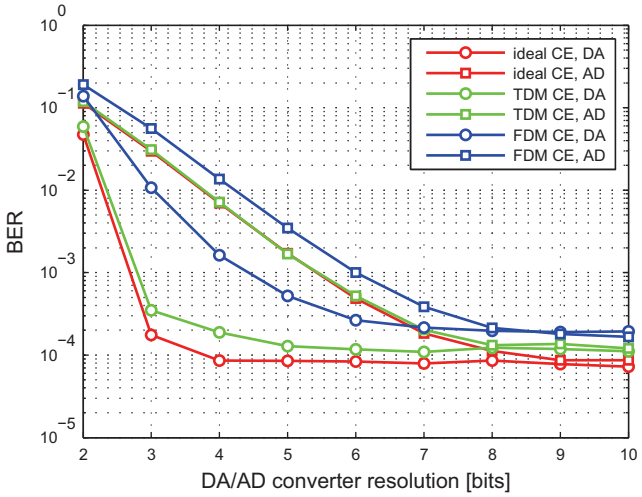


Figure 9: BER as a function of DA/AD converter resolution

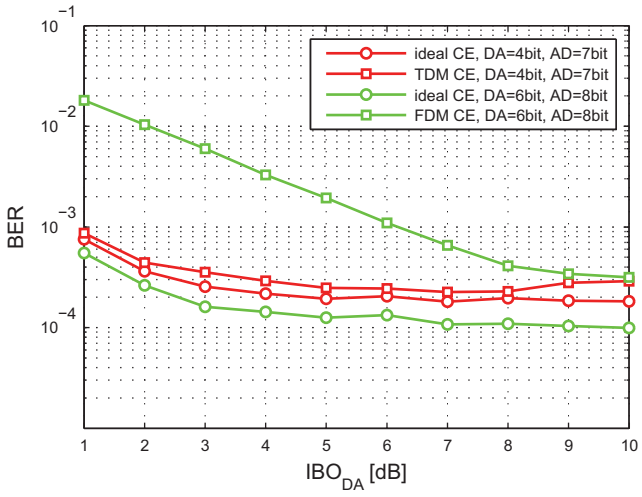


Figure 10: BER as a function of DA converter input back-off

The results also show the performance being more dependent on the resolution of DA converter, but one should be aware that an ideal AGC is considered at the receiver, thus guaranteeing minimum quantization error and no signal clipping at the receiver, while $IBO_{DA} = 10$ dB was selected at the transmitter. The latter is further analysed bellow.

### *IV.C The Impact of DA Converter Saturation Level*

The results provided in Sect. IV.A show, that the targeted BER performance can be achieved for the TDM-pilot CE scheme at DA and AD converter resolution equal to $4$ and $7$ bits, respectively. On the other hand, the system with the FDM-pilot CE scheme required $6$ and $8$ bit resolutions of DA and AD converters to guarantee a comparable performance. This is true for the analysis of the system, where DA converter input back-off level $IBO_{DA} = 10$ dB is taken as a parameter. The simulation results provided in Fig. 10 show both CE schemes sensitivity to $IBO_{DA}$ at the $E_b/N_0 = 35.0$dB. As a reference, curves corresponding to the system with equal DA and AD resolutions but ideal CE are also plotted. The results show that TDM-pilot CE scheme again outperforms the FDM-pilot based CE scheme. This can again be ascribed to constant amplitudes of pilot symbols in the case of TDM-pilot CE scheme, and clipped pilot symbols in the FDM-pilot CE scheme.

## V Conclusion

In this paper, we discussed and analysed a practical pilot assisted CE implementation in the OFDM system. In particular, the impact of DA and AD converters on TDM- and FDM-pilot CE schemes was investigated, with the results obtained for different bit resolutions and DA converter input back-off levels, but in all cases considering ideal AGC at the receiver. The TDM-pilot CE scheme emerged as more robust as compared to the FDM-pilot CE scheme, hence requiring lower DA and AD converter resolutions as well as lower input back-offs. This is mainly due to the fact that the probability of amplitude clipping at the transmitter and/or large quantization steps in the case of large signal amplitudes at the receiver is much higher in the case of FDM-pilot CE scheme, because its pilot symbols are unlike Chu sequence based TDM-pilot CE symbols are not characterised by a constant amplitude.

## References

[1] J. G. Proakis. *Digital communications*, 3rd ed. McGraw-Hill, 1995.

[2] S. Hara and R. Prasad. *Multicarrier Techniques for 4G Mobile Communications.* Artech House, June 2003.

[3] S. Coleri, M. Ergen, A. Puri, and A. Bahai. Channel estimation techniques based on pilot arrangement in OFDM systems *IEEE Transactions on Broadcasting*, Vol. 48, No. 3, pp. 362-370, September 2002.

[4] H. Schmidt and K.-D. Kammeyer. Quantization and its effects on OFDM concepts for wireless indoor applications. In *Proceedings of the 4th International OFDM-Workshop (InOWo 99)*, Hamburg, Germany, September 1999.

[5] X. Shao and C. H. Slump. Quantization Effects in OFDM Systems. In *Proceedings of the 29th Symposium on Information Theory*, pp. 93-103, Leuven, Belgium, May 2008.

[6] D. Dardari. Joint clip and quantization effects characterization in OFDM receivers. *IEEE Transactions on Circuits and Systems*, Vol. 53, No. 8, pp. 1741-1748, August 2006.

[7] H. Yang, T.C.W. Schenk, P.F.M. Smulders, E.R. Fledderus. Joint Impact of Quantization and Clipping on Single- and Multi-Carrier Block Transmission Systems. In *Proceedings of the IEEE Wireless Communications and Networking Conference 2008 (WCNC 2008)*, pp. 548-553, Las Vegas, USA, April 2008.

[8] M. Sawada, H. Okada, T. Yamazato and M. Katayama. Influence of ADC Nonlinearity on the Performance of an OFDM Receiver. *IEICE Transactions on Communications*, Vol. E89-B, No. 12, pp. 3250-3256, December 2006.

[9] B. Widrow, I. Kollar and L. Ming-Chang. Statistical Theory of Quantization. *IEEE Transactions on Instrumentation and Measurement*, Vol. 45, No. 2, pp. 353-361, April 1996.

[10] O. Edfors, M. Sandell, J.-J. van de Beek, S. K. Wilson and P. O. Borjesson. OFDM channel estimation by singular value decomposition. *IEEE Transactions on Communications*, Vol. 46, No. 7, pp. 931-939, July 1998.

[11] D. C. Chu. Polyphase codes with good periodic correlation properties. *IEEE Transactions on Information Theory*, Vol. 18, No. 4, pp. 531-532, July 1972.